

# Segregation in a Fluidized Binary Granular Mixture: Competition between Buoyancy and Geometric Forces

Leonardo Trujillo<sup>1</sup>, Meheboob Alam<sup>2,3</sup> and Hans J. Herrmann<sup>1,2</sup>

<sup>1</sup>*Laboratoire de Physique et Mécanique des Milieux Hétérogènes (UMR CNRS 7636),*

*École Supérieure de Physique et de Chimie Industrielles,*

*10 rue Vauquelin, 75231 Paris Cedex 05, France*

<sup>2</sup>*Institut für Computeranwendungen 1, Pfaffenwaldring 27, D-70569 Stuttgart, Germany*

<sup>3</sup>*Engineering Mechanics Unit, JNCASR, Jakkur Campus, Bangalore 560064, India*

(Dated: October 31, 2018)

Starting from the hydrodynamic equations of binary granular mixtures, we derive an evolution equation for the relative velocity of the intruders, which is shown to be coupled to the inertia of the smaller particles. The onset of Brazil-nut segregation is explained as a competition between the buoyancy and geometric forces: the Archimedean buoyancy force, a buoyancy force due to the difference between the energies of two granular species, and two *geometric* forces, one *compressive* and the other one *tensile* in nature, due to the *size-difference*. We show that inelastic dissipation strongly affects the phase diagram of the Brazil nut phenomenon and our model is able to explain the experimental results of Brey *et al.*[16].

PACS numbers: 45.70.Mg;05.20.Dd

## I. INTRODUCTION

Segregation is a process in which a homogeneous mixture of particles of different species becomes spatially non-uniform by sorting themselves in terms of their size and/or mass [1, 2, 3, 4, 5, 6, 7]. Monte Carlo simulations of Rosato *et al.* [3] clearly demonstrated that the larger particles immersed in a sea of smaller particles rise to the top when subjected to strong vertical shaking. This is the well-known *Brazil nut phenomenon* (BNP). It has been explained using the geometrical ideas of *percolation* theory, *i.e.* in a vibrated-bed the smaller particles are more likely to find a void through which they can percolate down to the bottom, leaving the larger-intruder at the top[3, 8]. The *arching*-effects [4], whereby the larger particle is being supported by the arches of smaller particles, can help to assist the percolation-driven segregation. The second mechanism of segregation is the *convective* mean flow in the vibrated bed due to the formation of convective cells such that the particles move to the top through the central-axis[5]. Recently, another mechanism has been proposed, driven by the *inertia* of the intruder [6], which could explain the *reverse-buoyancy*-effect whereupon a *light* but large particle will sink to the bottom of a deep bed under *low-frequency* shaking. In Ref.[7], a buoyancy-driven segregation mechanism has been proposed, drawing a direct analogy with the standard buoyancy forces in a fluid. For other related issues on segregation, the reader is referred to the recent review article of Rosato *et al.*[2].

The interplay between size and mass has been considered by Hong *et al.*[9] who found that a downward intruders' movement occurs as well: *reverse Brazil nut phenomenon* (RBNP). They proposed a phase diagram for the BNP/RBNP transition, based on the competition between percolation and condensation. Recently, Jenkins and Yoon [10] investigated the upward  $\Leftrightarrow$  downward

transition employing the hydrodynamic equations for binary mixtures. The driving mechanism for segregation in the hydrodynamic framework is presumably different from that of the percolation-condensation idea and remains unexplained so far.

Employing the Enskog-corrected hydrodynamic equations for binary mixtures[11], we investigate the Brazil-nut segregation in a dry fluidized granular mixture in the absence of bulk convection. The purpose of this paper is three-fold: firstly, to derive a time-evolution equation for the relative velocity of a single intruder, taking into account the non-equipartition of granular energy; secondly, to explain the driving mechanism for Brazil-nut segregation in terms of the *buoyancy* and *geometric* forces. Lastly, based on a simple model for energy non-equipartition, we will show how the inelastic dissipation determines the regimes of BNP and RBNP.

## II. HYDRODYNAMICS OF GRANULAR MIXTURES

The validity of the hydrodynamic approach even in the dense granular flows has recently been justified via the comparison of theory with various experiments[12]—here one has to be careful in choosing the appropriate constitutive model for pressure, viscosity, dissipation, etc. The constitutive model that we have used has been validated by performing MD simulations of binary mixtures[13]. We consider a binary mixture of slightly inelastic, smooth particles (disks/spheres) with radii  $r_i$  ( $i = l, s$ , where index  $l$  stands for large and  $s$  for small), mass  $m_i$  and number density  $n_i$ . The species mass density is  $\varrho_i(\mathbf{x}, t) = m_i n_i = \rho_i \phi_i$ , where  $\rho_i$  is the material density of species  $i$  and  $\phi_i$  is its volume fraction. The total mass-density,  $\varrho(\mathbf{x}, t)$ , and the total number-density,  $n(\mathbf{x}, t)$ , are just the sums over their respective species val-

ues. The dissipative nature of particle collisions is taken into account through the normal coefficient of restitution  $e_{ij}$ , with  $e_{ij} = e_{ji}$  and  $0 \leq e_{ij} \leq 1$ .

Assuming unidirectional flow ( $\mathbf{u}_i = (0, v_i(y, t), 0)$ ;  $\partial/\partial x = 0$ ,  $\partial/\partial z = 0$  and  $\partial/\partial y \neq 0$ ) and neglecting viscous stresses, the momentum balance equation for species  $i$  can be written as [11]

$$\rho_i \frac{\partial v_i}{\partial t} = -\frac{\partial p_i}{\partial y} - \rho_i g + \Gamma_i. \quad (1)$$

(Note that the mass balance equations are identically satisfied for unidirectional flows.) Here  $p_i$  is the *partial* pressure of species  $i$ , and  $g$  the gravitational acceleration acting along the negative  $y$ -axis;  $\Gamma_i$  is the momentum source term which arises solely due to the interactions between *unlike* particles and  $\sum_{i=l,s} \Gamma_i = 0$  [11]. The assumption of negligible viscous stresses is justified if there is no overall mean flow in the system, or if the spatial variation of  $v_i(y, t)$  is small.

To obtain constitutive relations for partial pressures we take into account the breakdown of equipartition of energy between the two species (in the equation of state) as found in many recent theoretical and numerical studies[7, 11, 13, 14] and also confirmed in vibrofluidized experiments[15]. We assume that the single particle velocity distribution function of species  $i$  is a Maxwellian at its own granular energy  $T_i$ , where  $T_i = \frac{m_i}{d} \langle \mathbf{C}_i \cdot \mathbf{C}_i \rangle$ , with  $d = 2$  and  $3$  for disks and spheres, respectively,  $\mathbf{C}_i = \mathbf{c}_i - \mathbf{u}$  being the peculiar velocity,  $\mathbf{c}_i$  the instantaneous particle velocity and  $\mathbf{u} = \rho^{-1} \sum_{i=l,s} \rho_i \mathbf{u}_i$  the mixture velocity. The equation of state for the partial pressure of species  $i$  can then be written as:

$$p_i = n_i Z_i T_i, \quad \text{with} \quad Z_i = 1 + \sum_{j=l,s} K_{ij}. \quad (2)$$

Here  $Z_i$  is the *compressibility* factor of species  $i$  and  $K_{ij} = \phi_j g_{ij} (1 + R_{ij})^d / 2$ , with  $g_{ij}$  being the radial distribution function at contact and  $R_{ij} = r_i/r_j$  the size-ratio. Note that the  $K_{ij}$  are related to the collisional component of the partial pressure, having a *weak* dependence on inelasticity which we neglect, and  $Z_i \rightarrow 1$  in the dilute limit  $\phi \rightarrow 0$ . We shall return back to discuss more about the compressibility factor later.

After some algebraic manipulations with the momentum balance equations and the equation of state, we obtain the following evolution equation for the relative velocity of the larger particles,  $v_l^r = v_l - v_s$ ,

$$\rho_l \frac{\partial v_l^r}{\partial t} = n_l \left[ m_s \left( \frac{Z_l T_l}{Z_s T_s} \right) - m_l \right] g + \left[ 1 + \frac{p_l}{p_s} \right] \Gamma_l + p_l \frac{\partial}{\partial y} \left[ \ln \left( \frac{p_s}{p_l} \right) \right] - \rho_s \left( \frac{\rho_l}{\rho_s} - \frac{p_l}{p_s} \right) \frac{\partial v_s}{\partial t}. \quad (3)$$

An explicit expression for the momentum source term,  $\Gamma_l$ , can be obtained using the Maxwellian velocity distri-

bution function [11].

$$\Gamma_l = n_l K_{ls} T \left[ \left( \frac{m_s - m_l}{m_{ls}} \right) \frac{\partial}{\partial y} (\ln T) + \frac{\partial}{\partial y} \left[ \ln \left( \frac{n_l}{n_s} \right) \right] + \frac{4}{r_{ls}} \left( \frac{2m_l m_s}{\pi m_{ls} T} \right)^{1/2} (v_s - v_l) \right], \quad (4)$$

where  $T = n^{-1} \sum_{i=l,s} n_i T_i = \sum_{i=l,s} \xi_i T_i$  is the *mixture* granular energy,  $\xi_i = n_i/n$  the number-fraction of species  $i$ ,  $m_{ls} = m_l + m_s$  and  $r_{ls} = r_l + r_s$ . With additional assumptions of weak gradients in species number densities and granular energy, and retaining terms of the same order in the single intruder limit ( $n_l \ll n_s$ ), the evolution equation can be considerably simplified to

$$m_l \frac{dv_l^r}{dt} = \left[ m_s \left( \frac{Z_l T_l}{Z_s T_s} \right) - m_l \right] g - \frac{4K_{ls} T}{r_{ls}} \left( \frac{2m_l m_s}{\pi m_{ls} T} \right)^{1/2} v_l^r + \left[ m_s \left( \frac{Z_l T_l}{Z_s T_s} \right) - m_l \right] \frac{dv_s}{dt}. \quad (5)$$

This is our time-evolution equation for the relative velocity of a single intruder: the first term on the right hand side is the net gravitational force acting on the intruder, the second term is a ‘Stokesian-like’ drag force and the third term represents a weighted *coupling* with the inertia of the smaller particles. It is interesting to recall the work of Shinbrot and Muzzio[6] who argued that the onset of reverse-buoyancy would crucially depend on the inertia of the smaller particles—a detailed analysis of eq. (5) with appropriate boundary conditions is left out for a future investigation. In this paper, we are only interested in the *steady-state* solution of the above equation. In typical situations where one can neglect the last term (e.g. if the intruder is much heavier than the smaller particles), we end up with the familiar evolution equation where the inertia of the intruder is being balanced by the net gravitational force and the drag force. Only in this case, the interplay between the gravitational and drag force will eventually decide whether the intruder rises or sinks. Neglecting transient effects, the steady relative velocity of the intruder can be obtained from

$$v_l^r = \frac{r_{ls} g}{4K_{ls}} \left( \frac{\pi m_{ls}}{2m_l m_s T} \right)^{1/2} \left[ m_s \left( \frac{Z_l T_l}{Z_s T_s} \right) - m_l \right]. \quad (6)$$

Setting this relative velocity to zero, we obtain the criterion for the *transition* from BNP to RBNP:

$$m_s \left( \frac{Z_l T_l}{Z_s T_s} \right) - m_l = 0, \quad (7)$$

which agrees with the expression of Jenkins & Yoon[10] for the case of equal granular energies ( $T_l = T_s$ ). As such, it is not evident from this expression *what the driving mechanism for segregation is*. Thus, we need to answer several questions. Can we recast the segregation criterion in terms of the well-known Archimedean and thermal buoyancy forces? Is there any new force, and what could be the physical origin of such forces?

### III. DRIVING MECHANISM: SEGREGATION FORCES

To understand the *origin* of segregation in the present framework, we now decompose the net gravitational force in eq. (5) for a *single* intruder in the following manner:

$$F = g \left[ (\rho_s - \rho_l)V_l + m_s \left( \frac{T_l}{T_s} - 1 \right) \frac{Z_l}{Z_s} + m_s \left( 1 - \frac{V_l}{V_s} \right) + m_s \left( \frac{Z_l}{Z_s} - 1 \right) \right], \quad (8)$$

where  $V_i$  is the volume of a particle of species  $i$ . The first term,  $F_B^A = V_l(\rho_s - \rho_l)g$ , is the effective Archimedean buoyancy force which arises due to the weight of the *displaced* volume of the intruder ( $V_l$ ). The second term,  $F_B^T \propto (T_l - T_s)$ , represents the buoyancy force due to the difference between the two species granular energies. This, being an *analog* of the thermal buoyancy, may be termed the *pseudo-thermal* buoyancy force.

There are two more terms in eq. (8) which do not appear to be related to standard buoyancy arguments. The third term is *negative definite*, and vanishes identically if the intruder and the smaller particles have the *same size*. Note that  $\epsilon_v^{st} = (V_l/V_s - 1)$  is the *volumetric* strain. Thus,  $F_{ge}^{st} = -m_s g \epsilon_v^{st}$  is a *static compressive* force to overcome the barrier of the *compressive* volumetric strain arising out of the *size-disparity* between the intruder and the smaller particles.

The fourth term in eq. (8),  $\propto (Z_l/Z_s - 1)$ , vanishes in the dilute limit  $\phi \rightarrow 0$ . It can be verified that  $(Z_l/Z_s - 1)$  also vanishes identically, irrespective of the total volume fraction, *if the particles are of the same size*. (Note that we have neglected the weak-dependence of  $Z_i$  on inelasticity.) Thus, the *origin* of this force is also tied to the *size-disparity* as in the third term  $F_{ge}^{st}$ . An interesting *physical* interpretation can be made if we consider the dense limit with a single intruder ( $\phi_l \ll \phi_s$ ):  $(Z_l/Z_s - 1) \propto R_{ls}^d$  for  $R_{ls} \gg 1$ . Hence  $\epsilon_v^{dyn} = (Z_l/Z_s - 1) \geq 0$  can be associated with a weighted *volumetric* strain, *tensile* in nature. Thus,  $F_{ge}^{dyn} = m_s g \epsilon_v^{dyn}$  is a *dynamic* tensile force that arises from the *excess* pressure difference due to the *nonideal* (collisional) interactions between the intruder and the *displaced* smaller particles.

Thus, the *geometric* effects due to the *size-disparity* contribute two new types of segregation forces:

$$F_{ge} = F_{ge}^{st} + F_{ge}^{dyn} = -m_s (\epsilon_v^{st} - \epsilon_v^{dyn}) g, \quad (9)$$

the former is a static, compressive force and the latter is a dynamic, tensile force. On the whole, the collisional interactions help to reduce the net compressive force that the intruder has to overcome.

A question naturally arises as to whether we could get back the standard Archimedes law from eq. (8) if we take the corresponding fluid limit, i.e. a large particle being immersed in a sea of small particles with  $r_l \gg r_s$ . In this limit it immediately follows that

$F_{ge}^{dyn} \rightarrow m_s(V_l/V_s - 1) = -F_{ge}^{st}$  and hence  $F_{ge} \equiv 0$ . Thus, the net gravitational force on a particle falling/rising in an otherwise quiescent fluid (at the same temperature) is nothing but the standard Archimedean buoyancy force,  $F = F_B^A = g(\rho_s - \rho_l)V_l$ . It is worth recalling that when there is *no* size-disparity ( $r_l = r_s$ ), the geometric forces are identically zero. Hence the behaviour of a heavier particle in a sea of equal-size lighter particles is similar to that of a particle in a fluid.

To clarify our segregation mechanism, we show the variations of different segregation forces with the size-ratio in Fig. 1 for the two-dimensional case of *equal density* particles ( $\rho_l = \rho_s$ ) in the single intruder limit ( $\phi_l/\phi_s = 10^{-8}$ ) at a total solid fraction of  $\phi = 0.7$ , with the restitution coefficient being set to 0.9. For illustrative purposes, we have calculated the energy ratio,  $T_l/T_s$ , (see the lower inset in Fig. 1) from the model of Barrat and Trizac[14]. For this case, the Archimedean buoyancy force is identically zero, and the total geometric force remains negative, as seen from the upper inset in Fig. 1. The pseudo-thermal buoyancy force is, however, positive. Thus, the competition between the pseudo-thermal buoyancy force and the geometric forces leads to a critical size-ratio above which the intruder will rise for this case. (For the corresponding purely elastic case ( $e = 1$  and  $F_B^T = 0$ ), the net force is  $F \equiv F_{ge} < 0$  and hence the larger particle will sink to the bottom.) This mechanism holds also for the more general case ( $\rho_l \neq \rho_s$  and  $F_B^A \neq 0$ ) for which the total buoyancy force ( $F_B = F_B^A + F_B^T$ ) competes with the geometric forces ( $F_{ge} = F_{ge}^{st} + F_{ge}^{dyn}$ ) to determine the transition from BNP to RBNP; the inclusion of dissipation merely affects the location of the transition point (see Fig. 2 and the discussion below, for details).

### IV. PHASE DIAGRAM AND DISCUSSION

A typical phase diagram in the single intruder limit ( $\phi_l/\phi_s = 10^{-8}$ ), delineating the regimes between BNP and RBNP, is shown in Fig. 2 for the two-dimensional case, with other parameters as in Fig. 1. (The qualitative features of the corresponding phase diagram for the three-dimensional case are similar.) Focussing on the purely elastic case ( $e = 1$ ), we note that a transition from BNP to RBNP can occur following two paths (denoted by two arrows), one along the *constant mass-ratio* with decreasing size-ratio and the other along the *constant size-ratio* with increasing mass ratio. In both cases, the Archimedean buoyancy force balances the net geometric forces at the transition point.

Comparison between the elastic ( $e = 1$ ) and inelastic ( $e = 0.9$ ) cases in Fig. 2 clearly shows that the non-equipartition of granular energy, responsible for the pseudo-thermal buoyancy force  $F_B^T$ , has a dramatic effect in reducing the regime of RBNP, and decreasing the value of  $e$  reduces the size of this regime further. For the case of a mixture with equal volume fractions ( $\phi_l = \phi_s$ ), however, the regime of RBNP is much larger as seen from

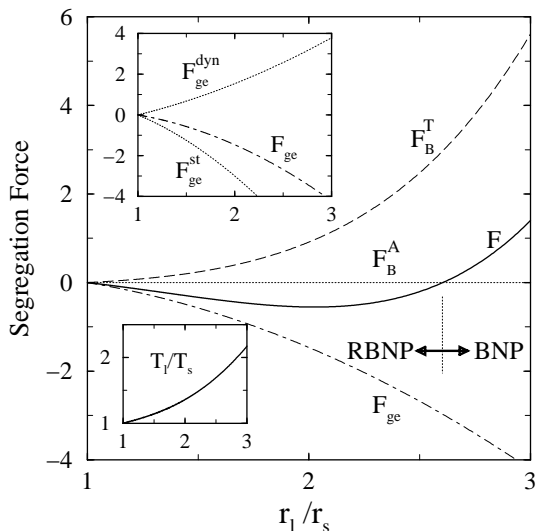


FIG. 1: Variations of segregation forces ( $F/m_s g$ ) with the size-ratio for  $\rho_l = \rho_s$  at  $e = 0.9$ ; see text for other details. The upper inset shows the corresponding static and dynamic contributions to the total geometric force ( $F_{ge} = F_{ge}^{st} + F_{ge}^{dyn}$ ). The lower inset shows the variation of  $T_l/T_s$  with the size-ratio[14].

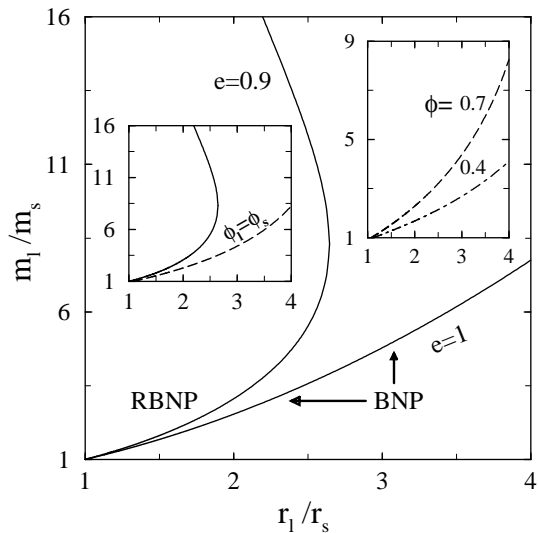


FIG. 2: Phase diagram for BNP/RBNP in two dimensions:  $\phi = 0.7$  and  $\phi_l/\phi_s = 10^{-8}$ . Left inset: phase diagram with  $e = 0.9$ ,  $\phi_l/\phi_s = 10^{-8}$  (solid curve) and  $\phi_l/\phi_s = 1$  (dashed curve). Right inset: phase diagram with  $e = 0.9$ ,  $\phi_l/\phi_s = 1$ ,  $\phi = 0.7$  (dashed curve) and  $\phi = 0.4$  (dot-dashed curve).

the left-inset of Fig. 2. This observation is in qualitative agreement with the recent experimental results of Breu *et al.*[16] who found that the ‘reverse Brazil-nut effect is completely destroyed if  $\phi_s \gg \phi_l$ ’.

The right-inset of Fig. 2 shows that the size of

the RBNP-regime also increases with decreasing overall mean volume fraction. Since in vibrated-bed experiments increasing the shaking amplitude is equivalent to decreasing the mean volume fraction, our observation explains another interesting result of Breu *et al.*[16] that for a given mixture with specified size- and mass-ratio, the final state is that of RBNP at sufficiently high accelerations (see Fig. 2 in Ref.[16]).

We need to point out that calculating the energy ratio ( $T_l/T_s$ , [14]) we made the assumption that  $e_{ij} = e$ . Using a variable restitution coefficient, our phase-diagram at large mass-ratios will be modified, but the proposed segregation mechanism and the qualitative features of the phase-diagram remain intact. Even though the model of Barrat & Trizac[14] is strictly valid for a homogeneous mixture with stochastic-driving, it has recently been verified in vibrofluidized-bed experiments under strong shaking[15].

To compare our segregation mechanism with others, we note that the scaling of the geometric forces ( $\propto R_{ls}^d$ ) suggests that they can be compared to the effective percolation force of Rosato *et al.*[3], and hence we have a competition between buoyancy and percolation forces. In the percolation-condensation mechanism of Hong *et al.*[9], the condensation is driven by the two-species having different energies. If one equates their driving force due to condensation-tendency with an effective buoyancy force, then our mechanism could be equivalent to that of Hong *et al.* However, there is no direct one-to-one analogy between our hydrodynamic segregation mechanism and the percolation-condensation mechanism.

In conclusion, we have identified four different types of segregation forces: apart from the Archimedean buoyancy force and an analog of the thermal buoyancy force, there are two additional forces, the origin of both is tied to the size-disparity between the intruder and the smaller particles. We have demonstrated that the competition between the buoyancy and geometric forces determines the onset of segregation in the present scenario, and the inclusion of the pseudo-thermal buoyancy force (due to inelastic dissipation) further enhances the possibility of BNP. While the possibility of RBNP is rather limited in the single intruder limit, even at moderate dissipation-levels, either increasing the relative volume fraction of the intruders or decreasing the mean volume fraction enhances its likeliness as in the experiments of Breu *et al.*[16].

## Acknowledgments

M.A. acknowledges the financial support from the AvH foundation, and discussions with Stefan Luding on related topics.

- 
- [1] H.J. Herrmann, J.-P. Hovi and S. Luding, *Physics of Dry Granular Media* (Kluwer, Dordrecht, 1998).
- [2] J. M. Ottino and D.V. Khakhar, *Annu. Rev. Fluid Mech.*, **32**, 55 (2000); A. Rosato et al., *Chem. Eng. Sci.*, **57**, 265 (2002).
- [3] A. Rosato et al., *Phys. Rev. Lett.* **58**, 1038 (1987); R. Jullien et al., *Phys. Rev. Lett.* **69**, 640 (1992).
- [4] J. Duran, J. Rajchenbach and E. Clément, *Phys. Rev. Lett.* **70**, 2431 (1993); S. Dippel and S. Luding, *J. Phys. I (Paris)* **5**, 1527 (1995).
- [5] J. B. Knight, H. M. Jaeger and S. R. Nagel, *Phys. Rev. Lett.* **70**, 3728 (1993); T. Pöschel and H. J. Herrmann, *Europhys. Lett.* **29**, 123 (1995).
- [6] T. Shinbrot and F.J. Muzzio, *Phys. Rev. Lett.* **81**, 4365 (1998). G. Gutiérrez et al., cond-mat/0211116.
- [7] L. Trujillo and H. J. Herrmann, *Physica A* (2003, in press), cond-mat/0202484; *Gran. Matt.* (2003, in press).
- [8] S. B. Savage and C. K. K. Lun, *J. Fluid Mech.* **194**, 457 (1988). N. Shishodia and C. R. Wassgren, *Phys. Rev. Lett.* **87**, 084302 (2001).
- [9] D.C. Hong, P.V. Quinn and S. Luding, *Phys. Rev. Lett.* **86**, 3423 (2001); J.A. Both and D.C. Hong, *Phys. Rev. Lett.* **88**, 124301 (2002).
- [10] J.T. Jenkins and D. Yoon, *Phys. Rev. Lett.* **88**, 194301 (2002).
- [11] J.T. Jenkins and F. Mancini, *J. Appl. Mech.* **54**, 27 (1987); J.T. Willits and B.Ö. Arnarson, *Phys. Fluids* **11**, 3116 (1999); M. Alam, J.T. Willits, B.Ö. Arnarson and S. Luding, *Phys. Fluids* **14**, 4085 (2002).
- [12] W. Losert, L. Bocquet, T.C. Lubensky and J.P. Golub, *Phys. Rev. Lett.* **85**, 1428 (2000); X. Yang et al., *Phys. Rev. Lett.* **88**, 044301 (2002).
- [13] M. Alam and S. Luding, *Gran. Matt.* **4**, 137 (2002); *J. Fluid Mech.* **476**, 69 (2003); Preprint (2003).
- [14] A. Barrat and E. Trizac, *Gran. Matt.* **4**, 57 (2002).
- [15] K. Feitosa and N. Menon, *Phys. Rev. Lett.* **88**, 198301 (2002).
- [16] A.P.J. Breu, H.-M. Ensner, C.A. Kruelle and I. Rehberg, *Phys. Rev. Lett.* **90**, 014302 (2003).